

Figure 1 – Load Recovery Index in three-point-bending for control specimens (TQ and MI series) and self-healing specimens (MS series).

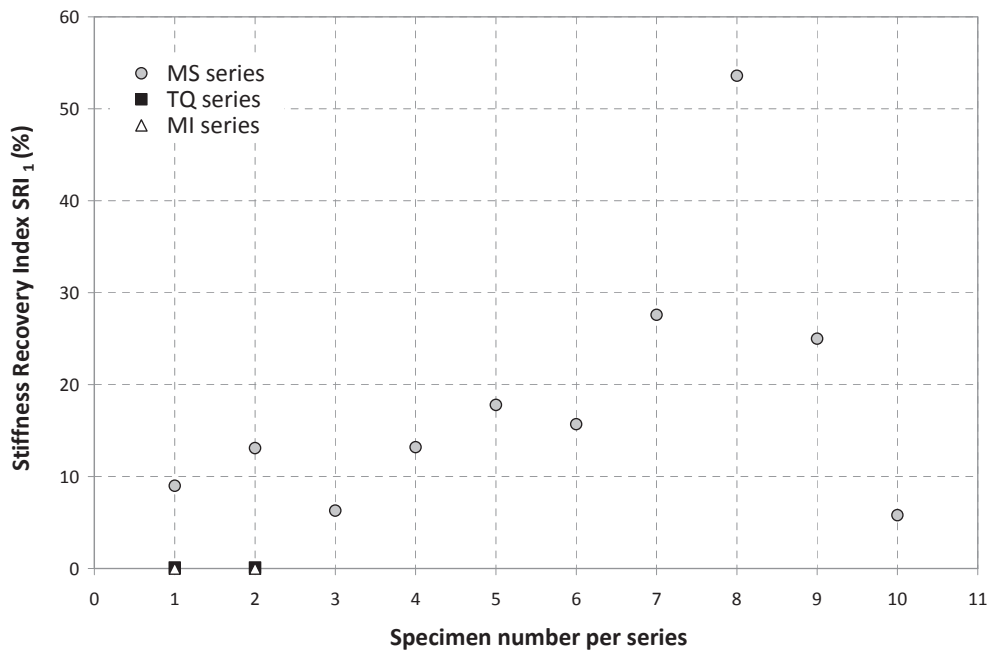


Figure 2 – Stiffness Recovery Index in three-point-bending for control specimens (TQ and MI series) and self-healing specimens (MS series).

INDIRECTLY-SUPPORTED ONE-WAY R/C SLABS: DURABILITY AND SAFETY ISSUES

Pietro G. Gambarova and Francesco Lo Monte

ABSTRACT: Simply-supported one-way R/C slabs are commonly used in the covers of small and medium underground facilities, where durability is the main issue face with rather limited service loads and short spans (2-4 m [6.5-13.0 ft]). The structural performance, however, should not be underrated, as being the slab in a roundabout does not prevent a heavy truck from straying off the right lane!

To have fresh information on durability and cracking (working loads), and on the bearing capacity and failure mode (ultimate loads), displacement-controlled tests have been recently performed in Milan on four typical rectangular R/C slabs suspended along their short sides via corbels (*dapped ends*; size: 1.3x2.2x0.15 m [51x87x6 in.]). A transversely-distributed or concentrated load was applied either at mid-span (in the bending tests), or at 1/10 of the span (in the shear tests).

The two slabs Type A are provided with longitudinal bent-up bars in the main body and hooks in the corbels. On the contrary, the slabs type B are reinforced via two continuous layers of longitudinal straight bars.

Under the working loads, cracking never occurred, neither in bending nor in shear – to the advantage of durability – while above the working loads rather complex crack patterns formed in the D zones close to the corbels, particularly under the concentrated load, which brought in 3-D effects, with a limited reduction in the bearing capacity.

Refining the reinforcement layout is shown – once more - to markedly improve slab performance, with little or no extra cost.

Keywords: cracking (in R/C), crack control, dapped ends, one-way slabs, R/C slabs, service loads, strut-and-tie systems, ultimate loads.

ACI member **Pietro G. Gambarova** is an Emeritus of Structural Engineering at the Department of Civil and Environmental Engineering of Politecnico di Milano, Milan, Italy, where he graduated in aeronautical engineering in 1966. He is active in FIB – Fédération International du Béton Task Groups 4.3 (Fire Design) and 4.5 (Bond Models). His research interests include shear and punching in reinforced concrete, plates and shells, bond mechanics, high-performance concrete, and fire design of R/C structures.

Francesco Lo Monte, is an associate researcher at the Department of Civil and Environmental Engineering of Politecnico di Milano, Milan, Italy, where he received his BS, MS and PhD (2014) degrees. His research interests include reinforced concrete mechanics, high temperature in R/C and innovative experimental techniques to monitor concrete spalling in fire. He is the winner of one of the three prizes awarded by ACI-Italy Chapter for the three best dissertations on structural concrete defended in the period 2012-14.

INTRODUCTION

The well-established use of R/C slabs or plates in the roofs of small-medium underground technical facilities and as temporary covers requires a proper design as the rather limited service loads (consisting in more or less thick soil and/or bituminous layers) do not rule out the transit of heavy vehicles when the building site is still open or in accidental situations (like in the case of a huge truck going off the road). In the latter case, the largest service loads per axle are 120 kN [27 kips] according to the Italian Highway Code, and 142 kN [32 kips] according to AASHTO^{1,2}.

Because of slabs simple geometry (with rectangular shape and uniform thickness in most cases), straightforward restraints (simple supports along two opposite sides and unidirectional bending) and moderate spans (2-4 m [6.5-13 ft]), however, the structural requirements are often underrated, and the reinforcement is often too light to the detriment of both durability and safety, particularly in the case of shallow corbels running along the short sides. In Fig.1 the layouts of four commonly-found bar arrangements are sketched: the layout A is the most efficient in both bending and shear, while the layout B is the simplest. The layouts A' and B' are modified versions of A and B, respectively.

The layouts A and B have been adopted in the slabs tested in this project, whose objectives are (a) to have fresh and direct information on cracking under the working loads (in bending and shear) and on the bearing capacity under the ultimate loads (in shear), (b) to check the reliability of the strut-and-tie systems proposed in the literature for shear (Type A Slabs), and of the equations provided by *fib* and ACI codes (Type B Slabs), and (c) to refine the strut-and-tie systems in order to properly introduce hook-concrete bond. (In this paper only the experimental results are presented and discussed).

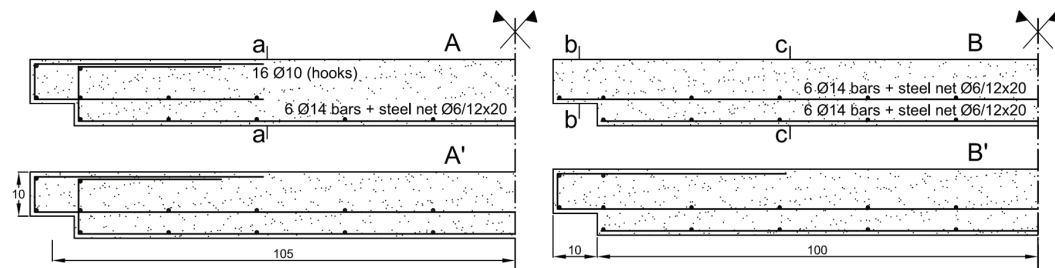


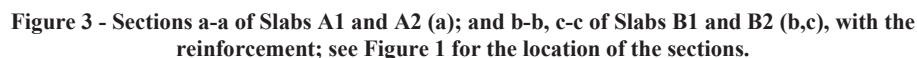
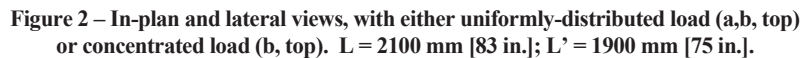
Figure 1 - Commonly-found bar layouts in R/C slabs simply-supported at two sides by means of corbels.

The four slabs tested in Milan (layouts A and B, Fig. 1) were loaded in bending up to the working loads (60 kN [13.5 kips]) equivalent to 120 kN [27 kips] per axle) and later in shear up to the ultimate loads (90 kN [20.2 kips]). However, the tests in shear were continued up to the peak load (= ultimate bearing capacity) and beyond, through the softening phase. The displacement-controlled tests were discontinued once the residual bearing capacity had fallen below 80% of the peak load.

For each bar layout two load situations were investigated, the first with the load distributed over the entire width of the slabs (Tests 1,2,5,6,9-12, Figs.2a,b) and the second with the load concentrated over 40% of the width (Tests 3,4,7,8, Fig.2b). In both cases, the loaded surfaces were designed to resist the maximum pressure specified by the Italian code¹ under the working loads (8 daN/cm² [116 psi]). The loaded surface was, therefore, a 1300x60 mm [51x2.4 in.] strip under distributed loading, and a 500x150 mm [19.7x5.9 in.] rectangle under concentrated loading. The amounts of the reinforcement in tension in the corbels and in the main body of the slabs are the same for both Type A and Type B slabs, even if the bar arrangement in the corbels is different in the two types of slabs. Furthermore, in both Type A and Type B slabs bar-concrete bond is crucial,

Note that the structural typology considered in this project is very usual as demonstrated by the many studies found in the literature^{3-5,7-12}, where various strut-and-tie systems have been developed (Type A Slabs), and by the design-oriented equations given in the codes (Type B Slabs)^{6,10}.

The reinforcement ratios at mid-span are $\rho = 0.73\%$ in Type A Slabs (effective depth $d = 128$ mm [5 in.]) and $\rho = 1.80\%$ in Type B Slabs ($d = 103$ mm [4 in.]), Figs.3a,b. The reinforcement ratios in the corbels are practically the same in Type A and Type B Slabs, with $\rho' = 1.14\%$ in the former case, and $\rho' = 1.19\%$ in the latter case, Fig.3c.



15.3

Test No.	Slab	Reinf.	Load	Test type	SLS/ULS	P _{max} (kN) [kips]
1	A1	HKD	UDL	BND	WLD	60.0 [13.5]
2	B1	STR	UDL	BND	WLD	60.0 [13.5]
3	A2	HKD	CNL	BND	WLD	60.0 [13.5]
4	B2	STR	CNL	BND	WLD	60.0 [13.5]
5	A1	HKD	UDL	SHR	PLD	401.0 [90.1]
6	B1	STR	UDL	SHR	PLD	172.2 [38.7]
7	A2	HKD	CNL	SHR	PLD	383.0 [86.1]
8	B2	STR	CNL	SHR	PLD	162.2 [36.5]
9	A1	HKD	UDL	SHR	PLD	286.5 [64.4] (*)
10	B1	STR	UDL	SHR	PLD	148.7 [33.4]
11	A2	HKD	UDL	SHR	PLD	426.2 [95.8]
12	B2	STR	UDL	SHR	PLD	174.2 [39.1]

HKD/STR = hooks and bent-up bars/straight bars in the slab and in the corbels

UDL/CNL = uniformly-distributed/concentrated load in the transverse direction

BND/SHR = test in bending/shear ; WLD/PLD = working load/peak load

(*) Test stopped at roughly 2/3 of the maximum expected load because of press malfunctioning.

LOADS AND INSTRUMENTATION

The first aim of the tests was to check the proper behaviors (a) in bending under the working loads (own weight + variable load up to 60 kN [13.5 kips] applied at mid-span); and (b) in shear under the ultimate loads (own weight + variable load $\geq 1.5 \times 60 = 90$ kN [20 kips] applied at 10% of the simply-supported span).

As mentioned in the Introduction, in four tests (Tests 1 and 2 in bending, 5, 6 and 9-12 in shear, Figs.2a,b) the load was distributed over the entire width of each slab, while in the other four tests (Tests 3 and 4 in bending; 7 and 8 in shear, Fig.2) the load was concentrated over 40% of the width. In all tests, the loaded surface was close to 2.8% of the total surface. As shown in Figs. 4a,b concerning two typical tests in bending and shear, the load was applied by means of one hydraulic jack (capacity 1000 kN [225 kips]) acting on very stiff spreaders consisting of rail stumps (length 1300 mm or 500 mm [51 in. or 20 in.]; width 150 mm [6 in.]).

In all the tests with the distributed load, a steel strip (6 mm [0.24 in.]-thick) and a neoprene strip were inserted between the rail stump and the slab to apply the load exactly over the nominal surface (1300x60 mm [51x 2.4 in.]) and to make the contact with the concrete as uniform as possible.

In all the tests with the concentrated load, only a neoprene layer was inserted in contact with the concrete, as the base of the rail stump had exactly the length and the width of the nominal contact surface (500x150 mm [20x6 in.]). In all cases, the thickness of the neoprene was 12mm [0.5 in.], and the subgrade stiffness was 0.50 MPa/mm [1.84 kips/in³].

The supports consisted in $\varnothing 40$ -mm [1.6 in.] steel bars; between these bars and the corbels a thick steel band ($t = 35$ mm [1.4 in.]) and a neoprene strip ($t = 12$ mm [0.5 in.]) were placed, the latter being necessary to equalize concrete roughness along the bottom face of the corbels. Both the band and the strip had in-plan dimensions equal to 1300x100 mm [51x4 in.].

All tests were displacement controlled (displacement rate of the piston of the hydraulic jack = 0.025 mm/s [0.001 in./s]). After a pre-loading cycle up to 15 kN [3.4 kips] (roughly 40% of the first-cracking load) to favor the settling of both the supports and the specimen, the load was increased by 10-15 kN at a time [2.2-3.3 kips] up to 60 kN [13.5 kips] in the bending tests and to 90 kN [20.2 kips] in the shear tests. (Of course, after each test in bending the specimens were unloaded and prepared for the subsequent tests in shear). The tests in shear were continued up to the load peak (*ultimate load* P_u) and beyond, until the resisting capacity had decreased below 80% of the peak load. At this point the tests in shear were stopped.

The tests in bending were monitored by means of two sets of three medium-stroke LVDTs (max. displacement ± 20 mm [± 0.8 in.]) placed under the specimen along the unsupported sides at 1/4, 2/4 and 3/4 of the span, Fig.5a. A further LVDT was placed under the centroid of the loaded area (LVDT No. 7). Furthermore, four short-stroke LVDTs (± 10 mm [± 0.4 in.]) were arranged at 45° astride the bisectors of the internal angles of the corbels, along the unsupported sides (Fig.5b). In this way, the onset and propagation of possible inclined cracks could be detected. The tests in shear were monitored in the same way along the unsupported sides (at 1/10, 2/4 e 3/4 of the span, Fig.5c) and under the centroid of the loaded area (LVDT No. 7). Two sets of three short-stroke LVDTs were arranged also astride the bisectors of the internal angles of the corbel closest to the applied load (Fig.5d).

Last but not least, two further short-stroke LVDTs were mounted at the extremities of one of the corbels (in the bending tests) or of the corbel closest to the applied load (in the shear tests) – see Figs.5b,d, respectively – to measure the settling of the neoprene strip. (The settling of the neoprene strips has to be subtracted from the values of the vertical displacement yielded by the medium-stroke LVDTs).

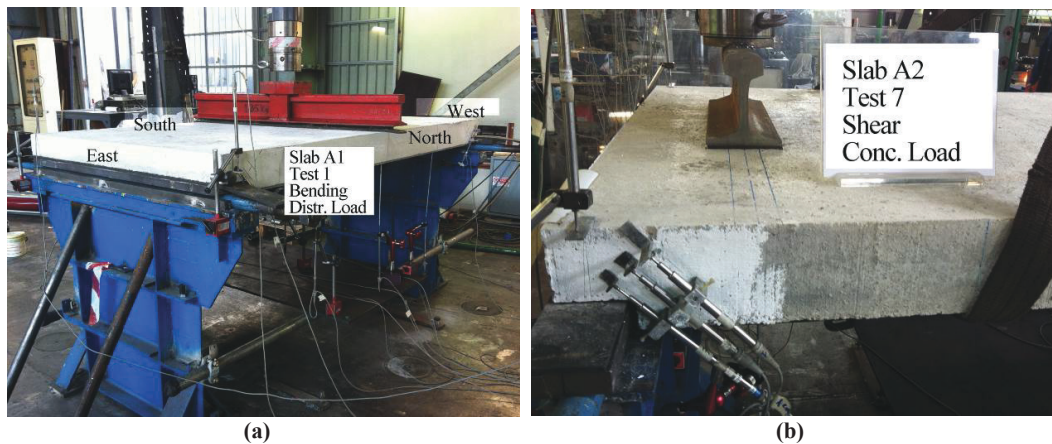


Figure 4 - Typical tests (a) in bending with distributed load (Slab A1, Test 1); and (b) in shear with concentrated load (Slab A2, Test 7).

Thirteen and fifteen LVDTs were used in each bending and shear test, respectively. The base-length and the spacing of the inclined LVDTs were close to 70 and 30 mm [2.8 and 12.0 in.], respectively.

The longitudinal displacements under the working loads (60 kN [13.5 kips]) are plotted in Fig. 6 for the four slabs investigated in this research project (Slabs A1 and B1 with distributed load, and A2 and B2 with concentrated load). Each diagram is the average of the measurements taken along each of the unsupported sides.

The diagrams are very similar, since in the uncracked regions ($M < M_{cr}$) there is hardly any difference (because of the negligible role of the reinforcement), while in the cracked regions ($M \geq M_{cr}$) the deformations are controlled by the bottom reinforcement, which is the same in all slabs. (Under the working loads, the intermediate reinforcement hardly contributes to the bending behavior of Slabs B1 and B2, because of the closeness of such reinforcement to the neutral axis of the sections).

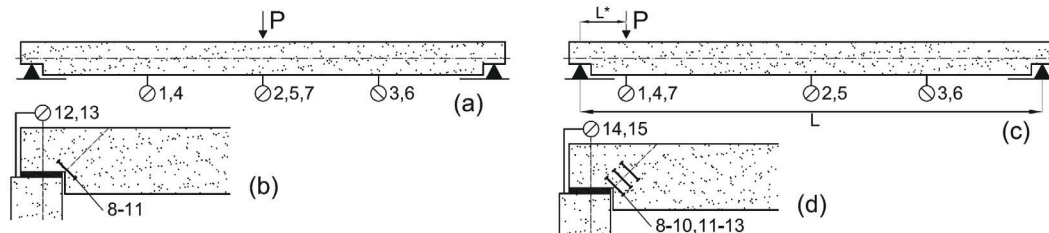


Figure 5 - Tests 1-8: bending tests (a,b) with 13 LVDTs (No.1-13); and shear tests (c,d) with 15 LVDTs (No.1-15). $L^* = 210$ mm [8.3 in.] in all tests.

BENDING TESTS AND VERTICAL DISPLACEMENTS

For the same arrangement of the reinforcement, the concentrated load yields a 20%-larger max. displacement in Slab A2 compared with Slab A1, and a 12%-larger max. displacement in Slab B2 compared with Slab B1. However, averaging the two load situations shows that straight bars (Slabs B1 and B2) bring in a very small increase (close to 4%) of the maximum displacement, compared with hooked bars (Slabs A1 and A2).

The reliability of the tests is confirmed by the regularity of the displacement curves. At mid span, the maximum moment M_{max} has reached the value 31.2 kNm [22.9 kips ft], higher than the first-cracking value ($M_{cr} = 20.8$ kNm [15.3 kips ft]), but lower than the ultimate resisting moment ($M_u = 72.3$ kNm [53.3 kips ft]) in Slabs A1 and A2; $M_u = 116.3$ kNm [85.7 kips ft] in Slabs B1 and B2).

As for cracking, no cracks appeared, neither at mid span (vertical cracks) nor at the inner corner of the corbels (inclined cracks), as demonstrated by the four inclined LVDTs (No.8-11, Fig.5b), which did not move. Under the working loads (60 kN [13.5 kips]), therefore, the proposed design for 2-2.5 m [6.5-8 ft]-span slabs efficiently contributes to durability, as no cracks appear.

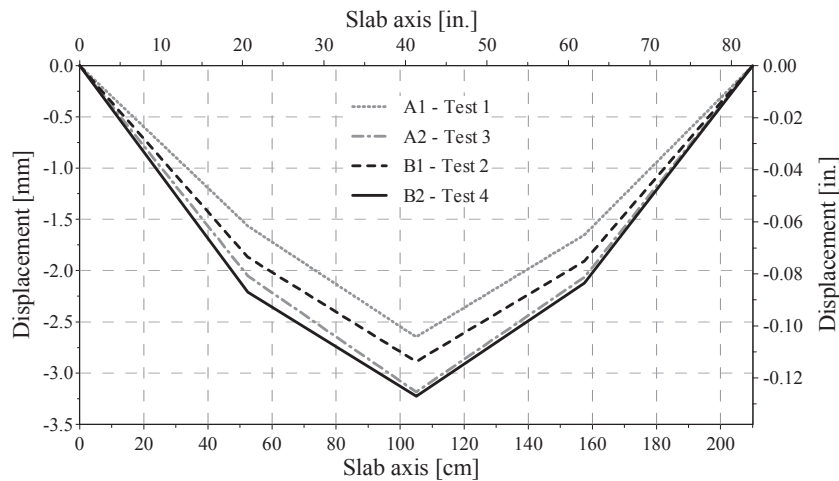


Figure 6. Bending tests (working loads): diagrams of the vertical displacement for the Slabs A1, A2 (hooks in the corbels and bent-up bars), and B1 and B2 (straight bars in two layers), for $P = 60$ kN [13.5 kips].

SHEAR TESTS AND LOAD-DISPLACEMENT DIAGRAMS

The load-displacement diagrams (with the displacement measured under the centroid of the load) are plotted in Figs. 7, 8 up to - and beyond - the peak load, until the resisting capacity has decreased by 20% compared with the peak load. In all diagrams, the values of the displacements were cleared of the settlements exhibited by the neoprene strips along the short sides. One may note:

- (a) the rather limited effect of transversely-distributed or concentrated loads:
- (a1) slabs with hooks and bent-up bars (Fig. 7): distributed load in Slabs A1 and A2 – Tests 5 and 11 ($P_{\max} = 414$ kN [93 kips] mean value) and concentrated load in Slab A2 – Test 7 ($P_{\max} = 383$ kN [86 kips]);
- (a2) slabs with straight bars (Fig. 8): distributed load in Slabs B1 and B2 – Tests 6, 10 and 12 ($P_{\max} = 165$ kN [37 kips] mean value) and concentrated in Slab B2 – Test 8 ($P_{\max} = 162$ kN [36.4 kips]);
- (b) the much greater ultimate capacity in the slabs provided with hooks and bent-up bars (Slabs A1 and A2, Tests 5, 7 and 11, $P_{\max} = 403$ kN [91 kips] mean value, Fig. 7) compared with the slabs with straight bars (Slabs B1 and B2, Tests 6, 8, 10 and 12, $P_{\max} = 164$ kN [37 kips] mean value, Fig. 8); in the former case, the ultimate capacity is roughly 2.5 times larger than in the latter case.

The slabs with straight bars (B1 and B2), however, exhibit a more ductile behavior (except Slab B2, Test 12), as more energy is dissipated by their complex crack system compared with the much stronger slabs reinforced with hooked bars (Slabs A1 and A2).

Last but not least, the initial slopes of the eight diagrams (Figs. 7 and 8) should be rather close, but this is true for Tests 5, 6, 8, 9, 10 and 12, while Tests 7 and 11 exhibit either a rather low or a rather high stiffness, respectively.

CRACK PATTERNS

In the bending tests, under the own weight and a mid-span distributed or concentrated load (which was increased step-by-step up to the service load of 60 kN [13.5 kips]) no cracks appeared in the discontinuity regions (Tests 1-4), as confirmed by the readings of the four inclined LVDTs, that remained stuck to zero. Even at mid-span, no bending-related cracks were observed along the bottom face, though the maximum moment ($M_{\max} = 31.2$ kNm [22.9 kips ft]) greatly exceeded the first-cracking moment ($M_{cr} = 20.8$ kNm [15.3 kips ft]). Note that the first-cracking moment was evaluated on the basis of the indirect strength in tension, in accordance with Model Code 90. In the shear tests (Tests 5-12, Figs. 9-12), no cracks appeared until the service load was reached, but later inclined cracks formed. In general, however, these *first cracks* hardly became the controlling factor of the ultimate behavior, as shown by Slab A2 – Test 7 (Fig. 11), where one of the first cracks radiating at roughly 45° from the apex of the angle stopped after the load had reached 90 kN [20 kips], while later a cracked band originating from the support formed and eventually prevailed.

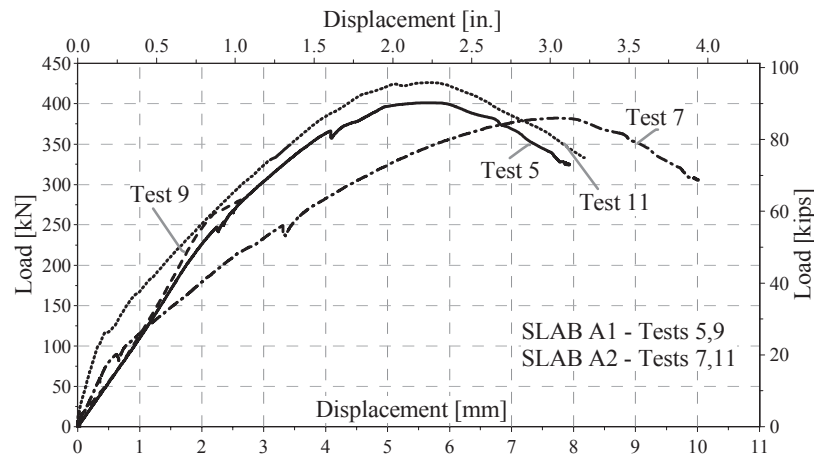


Figure 7 - Shear tests on Slabs A1 and A2 with hooks and bent-up bars: load-displacement diagrams of Tests 5, 9 and 11 under distributed load, and of Test 7 under concentrated load.

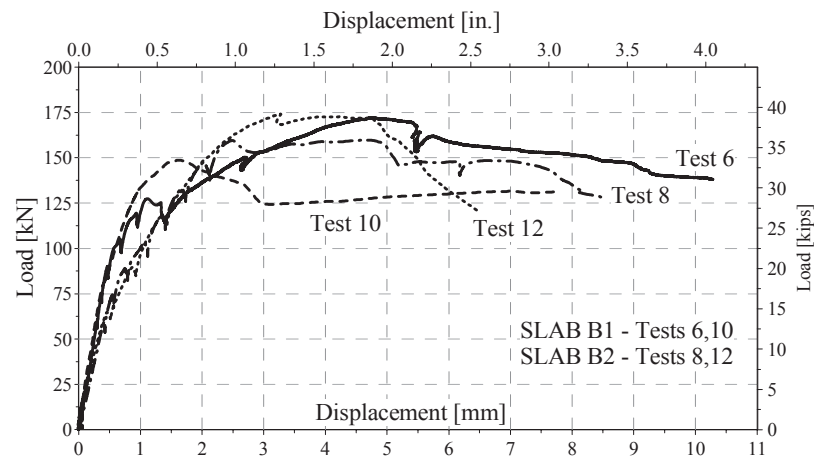


Figure 8 - Shear tests on Slabs B1 and B2 with straight bars: load-displacement diagrams of Tests 6,10 and 12 under distributed load, and of Test 8 under concentrated load.

Furthermore, in the slabs provided with web reinforcement (i.e. with vertical hooks and bent-up bars, Slabs A1 and A2, Figs. 9 and 11) the cracks turned out to be mostly inclined by 45° or were even steeper, but along the north side of Slab A2 (Fig. 11), where the initial cracks at 45° were accompanied by other flatter cracks certainly related to the 3D effects induced by the concentrated load, which was also responsible for the rather complex crack system visible along the top face.

In Slabs A1 and A2, the slope close to - or higher than -45° is justified by the formation of a strut-and-tie system (Fig. 13a), which becomes more and more evident under increasing loads and close to the collapse.

In Slabs B1 and B2 provided with straight bars (Figs. 10 and 12), the cracks tend to be flat and extended; furthermore, the concentrated load (Slab B2, Fig. 12) induces a 3D behavior that is the culprit of a complex system of cracks extending from the top surface to the unsupported sides. The rather flat alignment of the cracks is justified by the formation of a *shallow-arch and restraining-tie* system (Fig. 13b). The closer the collapse, the more evident the shallow-arch behavior.

In Figs. 14 and 15 the crack opening is plotted as a function of the load P , as measured by the instruments 11, 12 and 13 placed astride the bisector of the internal corner of the west corbel (north side, see Figs. 2a and 5d). The two figures refer to Tests 5 and 6 in shear (Fig. 2a) carried out on Slabs A1 (with hooks in the corbels and bent-up bars) and B1 (with straight bars), both uniformly loaded in the cross-wise direction. (Concentrated loads make the crack pattern three-dimensional and less understandable). Since the vertical and horizontal scales are different in Figs. 14 and 15, any comparison between the diagrams of the two figures requires some care.

Up to the service load ($P = 60 \text{ kN}$ [13.5 kips]), there are no visible cracks originating from the internal corner of the corbel (crack opening $\leq 50 \mu\text{m}$ in Slab A1, Fig.14 and $\leq 10 \mu\text{m}$ in Slab B1, Fig.15).

In Slab A1 (Fig.14) the opening of the single crack increases regularly with the load and tends to diverge – exhibiting very high values – starting from 90% of the maximum load (roughly 360 kN [80 kips] compared with 401 kN [90 kips]). The diagonal LVDTs were removed at roughly 90% of the expected maximum load to guarantee the integrity of the instrumentation against concrete splinters and chips. Note that the transverse reinforcement (bent-up bars) is rather effective in crack control up to high values of the cumulative width.

In Slab B1 (Fig.15), the cumulative width of the couple of inclined cracks exhibits very low values up to 50-55% of the maximum load (90 kN [20 kips] compared with 172 kN [38.7 kips]). The LVDTs were removed at 75% of the expected maximum load. Between 100 and 120 kN [22 and 27 kips], roughly 60 and 70% of the maximum load, crack opening tends to diverge at lower values than in the previous case (Fig.14), as a confirmation of the less efficient control exerted by straight bars on crack opening, to the detriment of durability.



Figure 9 - Slab A1 with hooks and bent-up bars: shear Test 5, distributed load, $P_u = 401 \text{ kN}$ [90 kips].



Figure 10 - Slab B1 with straight bars: shear Test 6, distributed load, $P_u = 172 \text{ kN}$ [39 kips].

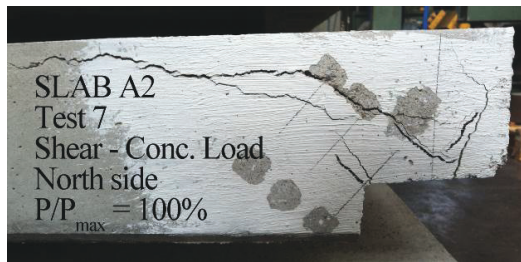


Figure 11 - Slab A2 with hooks and bent-up bars: shear Test 7, concentrated load, $P_u = 383 \text{ kN}$ [86 kips].

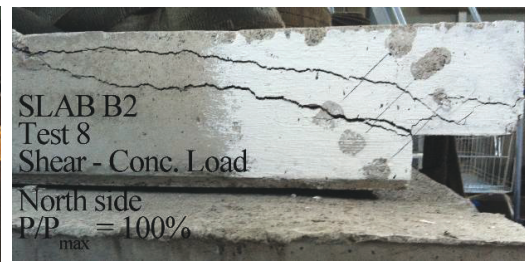


Figure 12 - Slab B2 with straight bars: shear Test 8, concentrated load, $P_u = 162 \text{ kN}$ [36 kips].

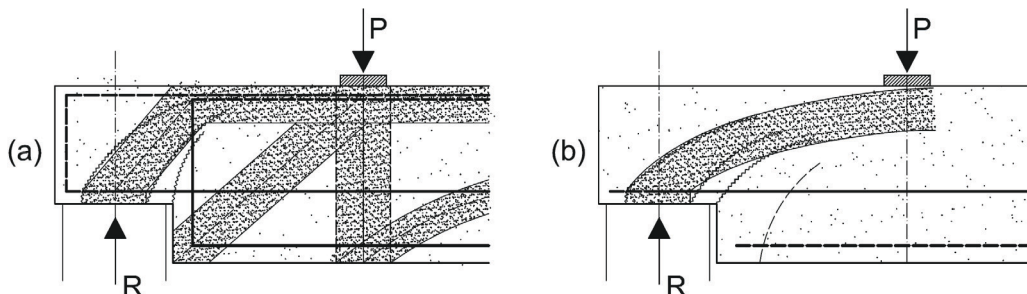


Figure 13 - Simplified behavior of dapped ends: (a) hooks and bent-up bars, and strut-and-tie system; and (b) straight bars and shallow-arch/restraining-tie system; concrete struts, ties and arches: dotted regions, enveloped by continuous or dashed lines; steel ties: heavy continuous lines; reinforcement axes: dashed lines. Last but not least, note that the diagrams referring to Slab B1 (Fig.15) exhibit sizeable load losses during the checks on the slab at prefixed values of the applied displacement. The load losses are indicated by the backward

jumps of the load, that are less evident in Slab A1 (Fig.14), most probably because cracking in this case is effectively controlled by the vertical arms of the bent-up bars reinforcing the slab.

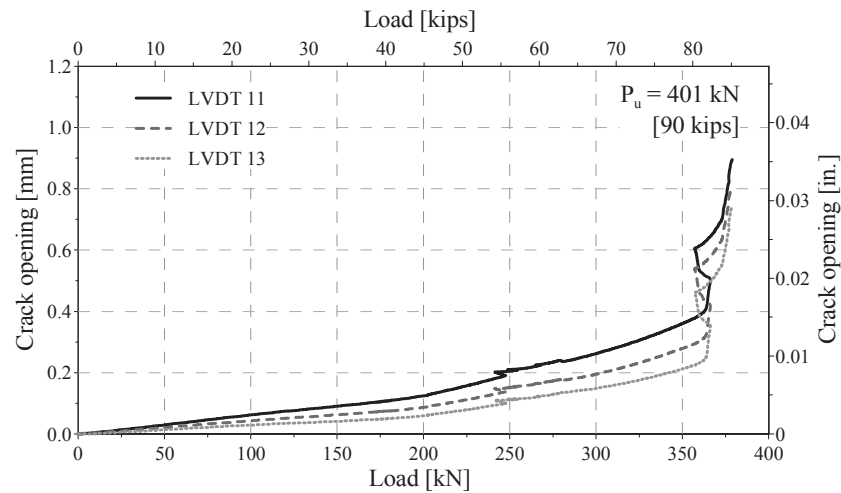


Figura 14 - Shear Test No.5 – Slab A1: cumulative crack width as a function of the load close to the internal corner of the corbel (west corbel, north side).

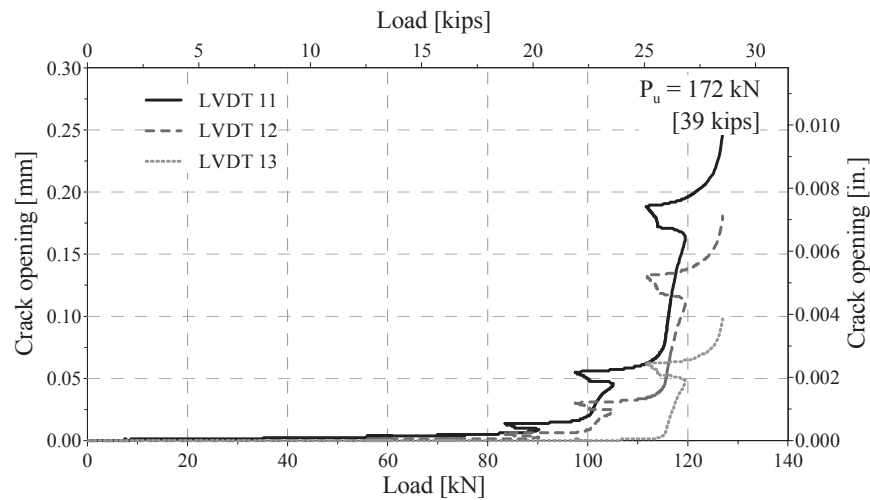


Figura 15 - Shear Test No.6 – Slab B1: cumulative crack width as a function of the load close to the internal corner of the corbel (west corbel, north side).

CONCLUDING REMARKS

Four rather usual rectangular uni-directional lightly-reinforced slabs simply-supported along the short sides by means of corbels (*dapped ends*) have been experimentally investigated in this project. The aim was to check their in-service and ultimate behaviors for two different reinforcement layouts (with/without hooks in the corbels and at the extremities of the longitudinal bars) and for two load distributions in the transverse direction. The four tests in bending under the working loads, and the eight tests in shear up to slab failure lead to the concluding remarks listed below.

- Under the working loads, the four slabs tested in 3-point bending behaved very well, with the load either uniformly distributed or rather concentrated in the transverse direction; there were no visible flexural cracks